Zebrafish live imaging reveals only around 2% rather than 50% of motor neurons die through apoptosis during development

Hao Jia [1], Hongmei Yang [1], Kathy Qian Luo [1,2] *

[1] Faculty of Health Sciences, University of Macau, Taipa, Macao SAR, China

[2] Ministry of Education Frontiers Science Center for Precision Oncology, University of Macau, Taipa, Macao SAR, China

*For correspondence: kluo@um.edu.mo

Abstract

It is widely accepted that neurons will die through apoptosis if they cannot receive enough growth factors during development of vertebrates; however, there is still no real-time observation showing this dying process in live animals. Here, we generated sensor zebrafish achieving live imaging of motor neuron apoptosis at single-cell resolution. Using these sensor zebrafish, we observed for the first time that in an apoptotic motor neuron, caspase-3 activation occurred quickly within 5-6 min and at the same time between the cell body and axon. Interestingly, we found that only around 2% of motor neurons died during zebrafish development, which is much lower than the generally believed 50% cell death occurred in embryonic stage of vertebrates. Our data also showed that most of the apoptotic bodies of these dead motor neurons were not cleared by macrophages. These sensor zebrafish can serve as powerful tools to study motor neuron apoptosis *in vivo*.

Introduction

Programmed cell death or apoptosis is a dynamic process that occurs in most tissues in live animals. In the nervous system, apoptosis plays an essential role in the regulation of neuronal cell numbers (Hollville, Romero, & Deshmukh, 2019). During embryonic development, a large number of neuronal cells die through apoptosis (Fuchs & Steller, 2011). In pathological states, such as Alzheimer's disease, Parkinson's disease, and motor neuron disease, the death of neuronal cells severely impairs the normal function of the nervous system (Butterfield & Halliwell, 2019; Michel, Hirsch, & Hunot, 2016; Moujalled, Strasser, & Liddell, 2021).

When apoptosis occurs, either through intrinsic or extrinsic pathways, it ultimately leads to the cascade activation of caspases and the degradation of cellular structures, which is no exception for neuronal cells (Blanquie et al., 2017; Heck et al., 2008; Hernandez-Baltazar, Mendoza-Garrido, & Martinez-Fong, 2013). Due to the unique and complex morphology of neuronal cells, especially long axons, many important issues related to neuronal cell apoptosis have not been fully addressed, including: (1) How to visualize neuronal cell death in live animals? (2) How fast caspase-3 can be activated within a single neuron during apoptosis? (3) Which part of a neuron (cell body vs. axon) will die first? To address these important questions, we need to develop novel tools that can monitor neuronal cell apoptosis in real time and in live animals.

Previously, we have developed a fluorescence resonance energy transfer (FRET)-based biosensor, named sensor C3, for detecting cancer cell apoptosis. Our *in vitro* results showed that sensor C3 could detect the apoptosis of cancer cells both in 2D and 3D cultures by changing its color from green to blue in real time (Anand, Fu, Teoh, & Luo, 2015; Fu, Peh, Ngan, Wei, & Luo, 2018; Hao, Huang, Wu, Peng, & Luo, 2023; K. Li, Wu, Zhou, Tong, & Luo, 2021; Luo, Vivian, Pu, & Chang, 2001; Tian, Ip, Luo, Chang, & Luo, 2007; Wu, Li, Yuan, & Luo, 2021;

Yang, Jia, Zhao, & Luo, 2022). Recently, we showed that sensor C3 could also be used to indicate zebrafish skin cell apoptosis (Jia, Song, Huang, Ge, & Luo, 2020).

In the present study, using *Tol2* transposon-based transgenic technology, we generated novel sensor zebrafish and achieved the real-time tracking of motor neuron apoptosis at single-cell resolution in live zebrafish. More importantly, using these sensor zebrafish, we were able to obtain novel insights into the spatiotemporal properties and occurring rates of motor neuron death during development.

Results

Generation of transgenic zebrafish expressing sensor C3 in motor neurons

Sensor C3 is a fusion protein of cyan fluorescent protein (CFP) and yellow fluorescent protein (YFP), between which is an amino acid linker containing the caspase-3 cleavage site DEVD (Figure 1A). In live cells, when sensor C3 is excited with a 458 nm laser, due to the energy transfer between CFP and YFP, the emission light of CFP can excite the YFP to emit green fluorescence, which can be detected at the wavelength of 535 nm. In apoptotic cells, activated caspase-3 proteins cleave sensor C3 at the DEVD site; due to the disruption of the FRET effect, sensor C3 emits blue fluorescence, which can be detected at the wavelength of 480 nm (Figure 1B).

In our previous publications, we have conducted many experiments to validate the specificity and sensitivity of sensor C3 for detecting caspase-3 activation and apoptosis. First, we confirmed that there was a strong energy transfer from CFP to YFP in purified sensor C3 proteins when CFP was excited. Second, we showed that the cleavage to sensor C3 is specific to caspase-3 and

requires the presence of the cleavage sequence of DEVD in sensor C3 proteins. Third, sensor C3 is highly sensitive to caspase-3 cleavage, as it could detect caspase-3 activation at a nanomolar concentration and in 5 min when sensor C3-labelled HeLa cells underwent UV irradiation-induced apoptosis (Luo et al., 2001).

We have confirmed that the apoptosis detected by sensor C3 was consistent with classical apoptotic assays, including chromatin condensation staining, caspase-3 activity assay, DNA fragmentation assay, and morphological changes such as cell shrinkage (Luo et al., 2001; Tian et al., 2007). Furthermore, we showed that sensor C3 could detect the apoptosis of various cancer cells and zebrafish skin cells by color change no matter the apoptosis was induced by UV irradiation, chemical drugs, fluidic shear stress, immune cells-mediated killing, or during normal development (Hao et al., 2023; Jia et al., 2020; K. Li et al., 2021; Luo et al., 2001; Tian et al., 2007; Yang et al., 2022). All aforementioned results show that sensor C3 is a very good tool for detecting apoptosis in live cells and animals.

To detect the death of motor neurons in live animals, we cloned sensor C3 under a motor neuron-specific promoter (Arkhipova et al., 2012) and used this construct to generate a transgenic line of sensor zebrafish Tg(*mnx1*:sensor C3) in which only the motor neurons specifically expressed sensor C3 proteins. After obtaining the sensor zebrafish, we first examined the morphology of motor neurons in zebrafish. At 33 hours post fertilization (hpf), we observed many green motor neurons inside the spinal cord (Figure 1C-D). More detailed observation revealed that approximately 10 motor neurons bundled together with their cell bodies located within the spinal cord, and their axons converged into one bundle to extend into individual somite, which serves as a functional unit for the development and contraction of muscle cells (Figure 1C-D).

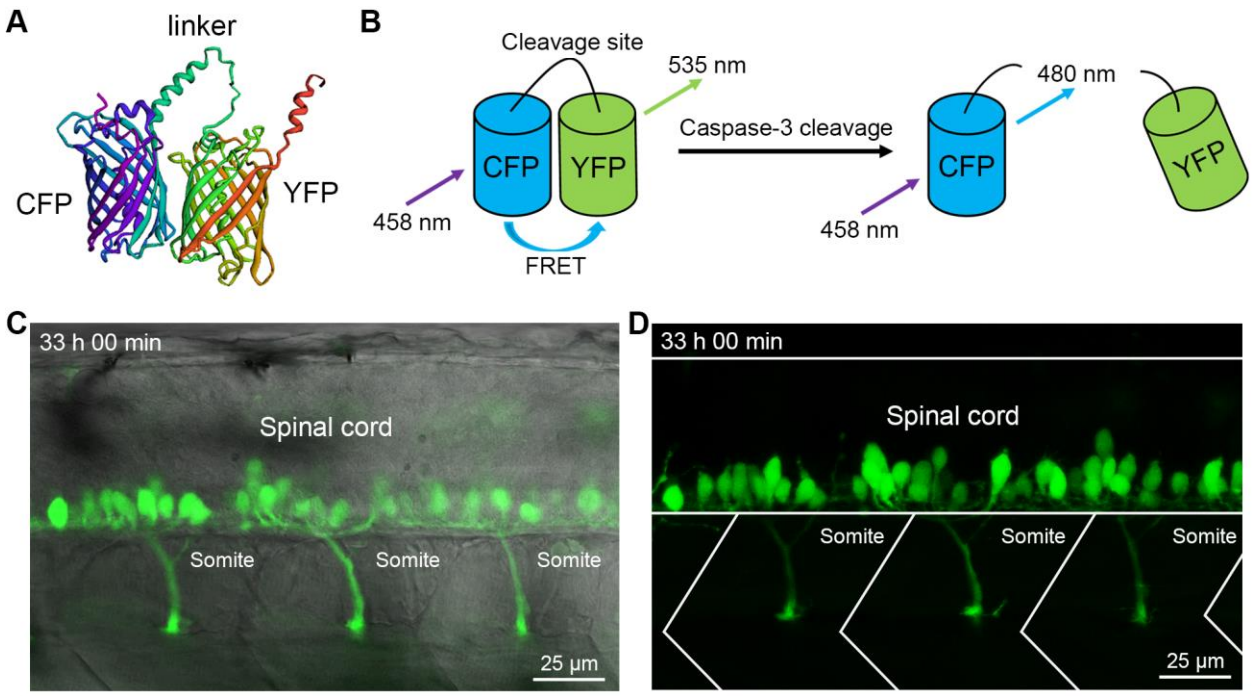

Figure 1. The live imaging of motor neurons in sensor zebrafish. (**A**) The structure of sensor C3 predicted by using Rosetta software. (**B**) The principle of sensor C3 for apoptosis detection. (**C-D**) The expression of sensor C3 in the motor neurons of Tg(*mnx1*:sensor C3) zebrafish. The bright field image and fluorescent image were merged in (C) to show the location of motor neurons and their axons. The anatomical structures and developmental time are indicated.

Both the cell body and axon of motor neurons can undergo apoptosis during zebrafish development

To determine the apoptotic status of motor neurons during the development, we took the images of CFP and YFP separately from the Tg(*mnx1*:sensor C3) zebrafish and merged them into FRET images. The green color will indicate the motor neurons are alive, and the blue color will indicate the neurons are apoptotic. The FRET imaging analysis showed that around 30 hpf during

zebrafish early development, the cell bodies of some motor neurons appeared in blue. In contrast, most of the cell bodies of these motor neurons appeared in green. Furthermore, the blue signals were also observed in the axon bundle of the motor neurons (Figure 2A-C). Image stacks of the apoptotic motor neuron in Figure 2C at different optical section levels better illustrated the blue signals in the axon region (Figure 2D). This observation indicates that the majority of the motor neurons are alive, and the minority can undergo apoptosis. Furthermore, both the cell body and axon of the motor neurons can undergo apoptosis during the early development of zebrafish.

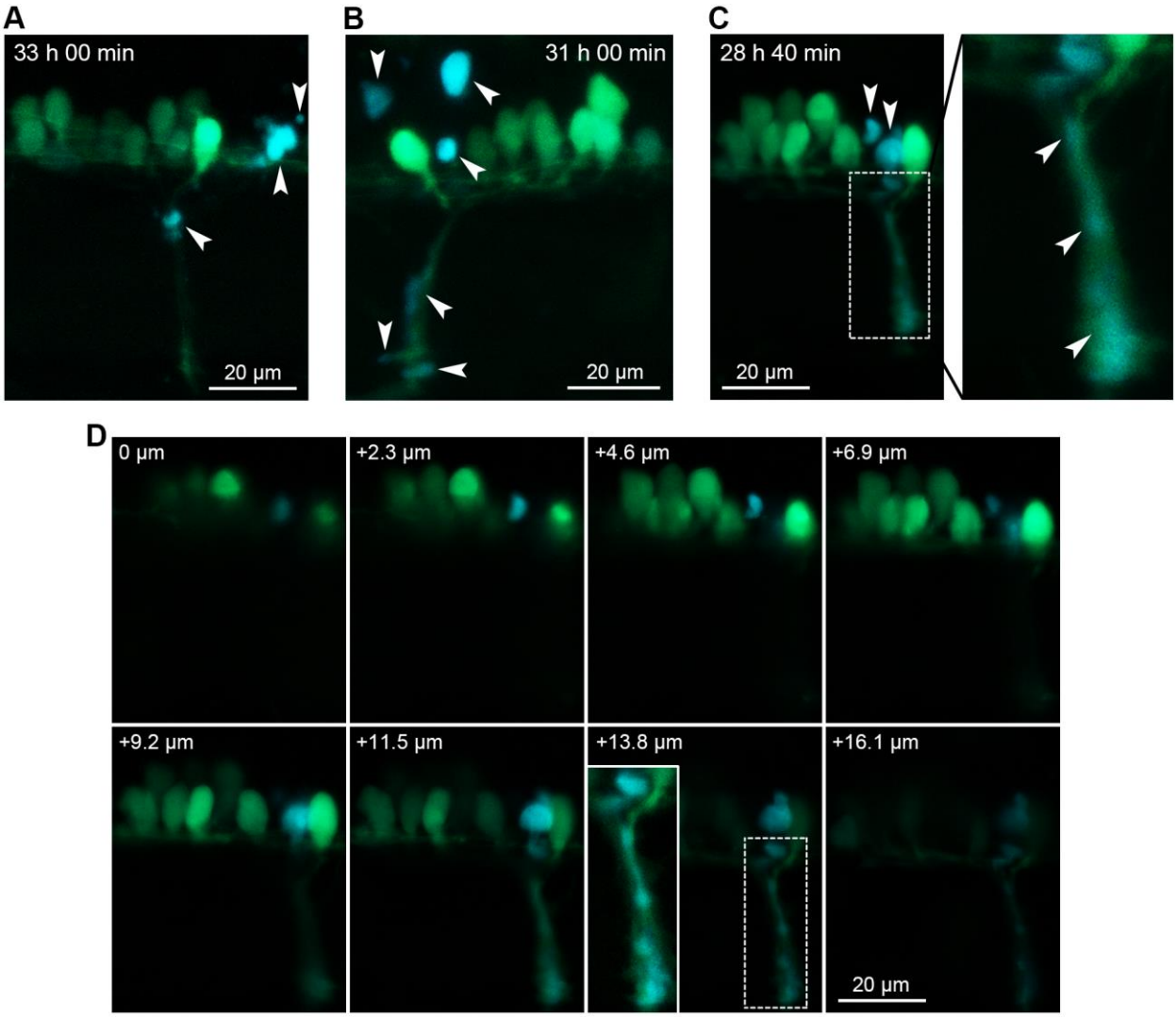

Figure 2. Both the cell body and axon of motor neurons can undergo apoptosis during zebrafish development. (**A**-**C**) FRET images of three somites showing motor neurons underwent apoptosis during the development of Tg(*mnx1*:sensor C3) zebrafish. The axon in (C) is enlarged for a better illustration. Blue apoptotic signals from cell bodies and axons are indicated with arrowheads. The developmental time is indicated in each image. (**D**) Z-stack imaging showed the apoptosis of the motor neuron in (C). The axon region in the stack of 13.8 μm is enlarged for a better illustration. The depth of each stack is indicated in each image.

The apoptosis of motor neurons occurred quickly and almost at the same time between the cell body and axon

Images in Figure 2 showed that blue signals appeared in both the cell body and axon of apoptotic motor neurons. To determine which part of a motor neuron died first and how fast the dying process was, we performed time-lapse imaging of caspase-3 activation in live zebrafish. FRET images in Figure 3A showed that at 32 h 15 min of zebrafish development, both the cell body (indicated with a white arrowhead) and the axon (indicated with a yellow arrowhead) of the indicated motor neuron were green, suggesting that caspase-3 was not activated. Just 3 min later, both the cell body and the axon started to change color (32 h 18 min). Another 3 min later, both the cell body and the axon became blue (32 h 21 min). At 32 h 27 min, two blue apoptotic bodies could be observed in the cell body region and multiple apoptotic bodies were also observed in the axon region. In the next 12 min (until 32 h 39 min), this apoptotic motor neuron gradually degraded into more and smaller apoptotic bodies (Figure 3A; Video S1).

The time-lapse imaging of another apoptotic motor neuron showed similar results (Figure 3B; Video S2). The color of both the cell body and axon of the motor neuron changed from green to blue within 5 min (from 30 h 45 min to 30 h 50 min). This apoptotic motor neuron gradually degraded into apoptotic bodies in the next 15 min (from 30 h 50 min to 31 h 05 min). These images showed that the activation of caspase-3 can occur within 5-6 min in both the cell body and axon of an apoptotic motor neuron. Thus, we conclude that the cell body and axon of the same motor neuron can undergo apoptosis at the same time during zebrafish development.

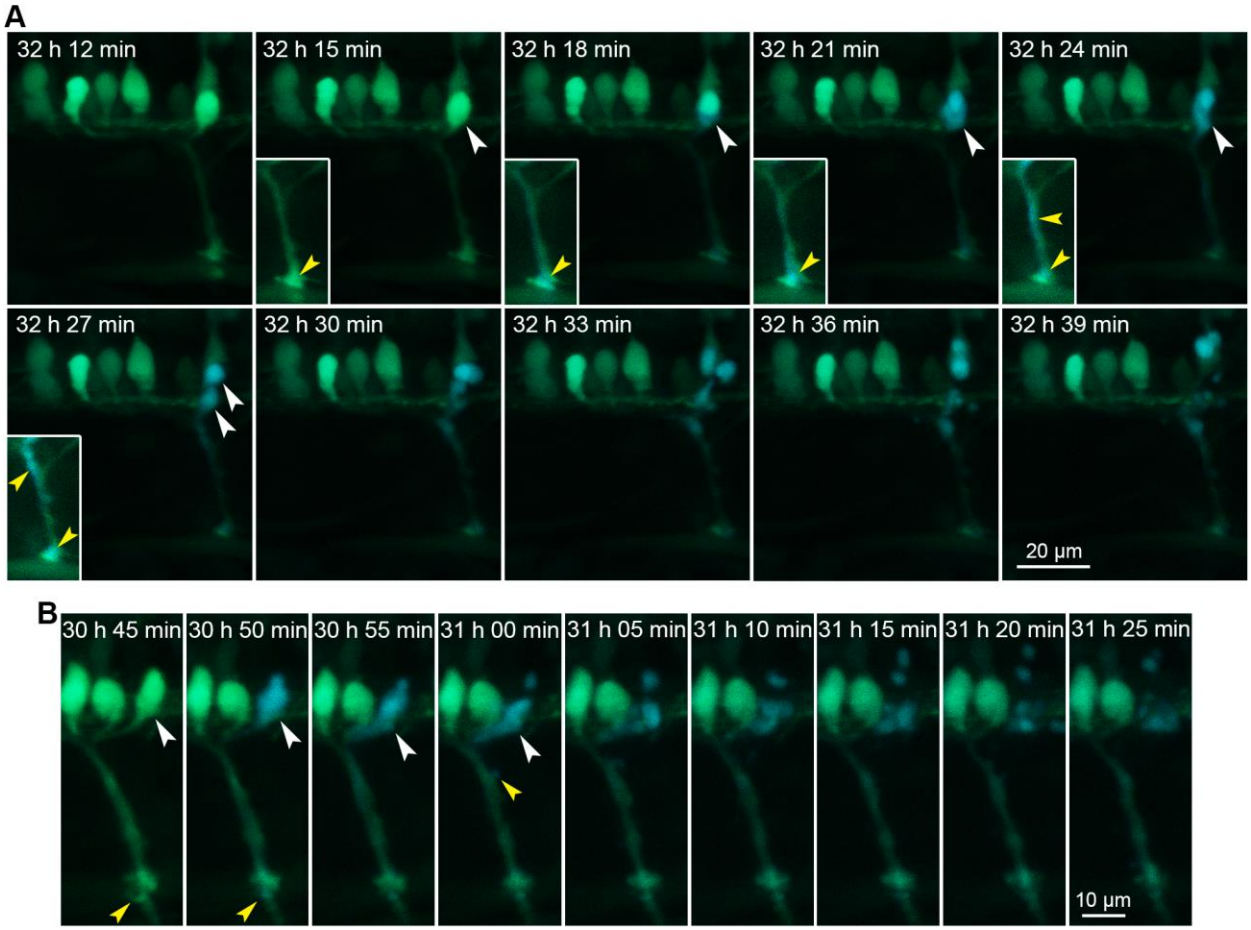

Figure 3. The apoptosis of motor neurons occurred quickly and almost at the same time between the cell body and axon. (**A**) Real-time imaging of motor neuron apoptosis during zebrafish development. During tracking, one motor neuron changed from green to blue. The cell body is

indicated with white arrowheads. The axon is enlarged for a better illustration and indicated with yellow arrowheads. The developmental time is indicated in each image. (**B**) Real-time imaging of the apoptotic process in another motor neuron during zebrafish development. The cell body is indicated with white arrowheads, and the axon is indicated with yellow arrowheads. The developmental time is indicated in each image.

Only around 2% of motor neurons died during zebrafish development

In the last several decades, the neurotrophic factor hypothesis has been widely accepted; that is, during the development of vertebrates, approximately 50% of neuronal cells in various regions of the nervous system will die if they cannot receive enough growth factors from their target cells (Castillo-Ruiz, Hite, Yakout, Rosen, & Forger, 2020; Dekkers, Nikoletopoulou, & Barde, 2013; Kandel, Schwartz, Jessell, Siegelbaum, & Hudspeth, 2012; Lossi & Merighi, 2003; Rubin, 1997). Regarding motor neuron development, chick embryos have served as the most studied models. Previous studies showed that half of motor neurons in the spinal cord died between day 5 to day 10 of incubation during the development of chick embryos (Hamburger, 1975; Oppenheim, 1981; Weill, 1991). Similar motor neuron death rates were also obtained between embryonic day 15 to day 18 during the development of rats (Harris & McCaig, 1984; Raoul, Henderson, & Pettmann, 1999; Weill, 1991).

Here, we counted the number of apoptotic motor neurons from 24 hpf to 120 hpf, which covers the major time window of neurogenesis during zebrafish development (Kaslin & Ganz, 2020; Schmidt, Strähle, & Scholpp, 2013) and found that the apoptosis of motor neurons mainly occurred between 24–48 hpf and peaked between 30–36 hpf (Figure 4A). Interestingly, this time window coincided with the time period during which spontaneous muscle twitches occurred in

zebrafish (Menelaou et al., 2008; Naganawa & Hirata, 2011). There may be some unknown connection between motor neuron apoptosis and spontaneous muscle twitches, which requires further investigation. Unexpectedly, only a tiny portion (1.6% at 30 hpf and 1.0% at 36 hpf) of the motor neurons underwent apoptosis (Figure 4B), which is much lower than the previous reports that approximately 50% of motor neurons were removed through apoptosis during early development of vertebrates.

To validate these results, we performed terminal deoxynucleotidyl transferase dUTP nick end labeling (TUNEL) assays in zebrafish frozen sections. The motor neurons of the sensor zebrafish were identified by immunofluorescence staining using an anti-GFP antibody plus a secondary antibody conjugated with a green dye, and the apoptotic motor neurons were detected by red TUNEL signals (Figure 4C). We analyzed 1,045 motor neurons at 30 hpf, 13 of which were TUNEL-positive, with an apoptotic rate of 1.2%. We also analyzed 652 motor neurons at 36 hpf, 5 of which were TUNEL-positive, with an apoptotic rate of 0.8% (Figure 4D). These results showed that the low apoptotic rates detected by sensor C3-based FRET imaging could be confirmed by the conventional TUNEL assays.

Previous studies showed that neurotrophic factors glial cell-derived neurotrophic factor (GDNF) and brain-derived neurotrophic factor (BDNF) were critical for the survival of motor neurons (Cintrón-Colón, Almeida-Alves, Boynton, & Spitsbergen, 2020; He, Zhang, Yung, Zhu, & Wang, 2013; Kishino, Ishige, Tatsuno, Nakayama, & Noguchi, 1997). Thus, we used morpholinos targeting GDNF and BDNF genes, respectively, to reduce the expression of these two genes. However, we did not observe significant increases in the number of apoptotic motor neurons after the knockdown of these two genes, respectively (Figure 4E).

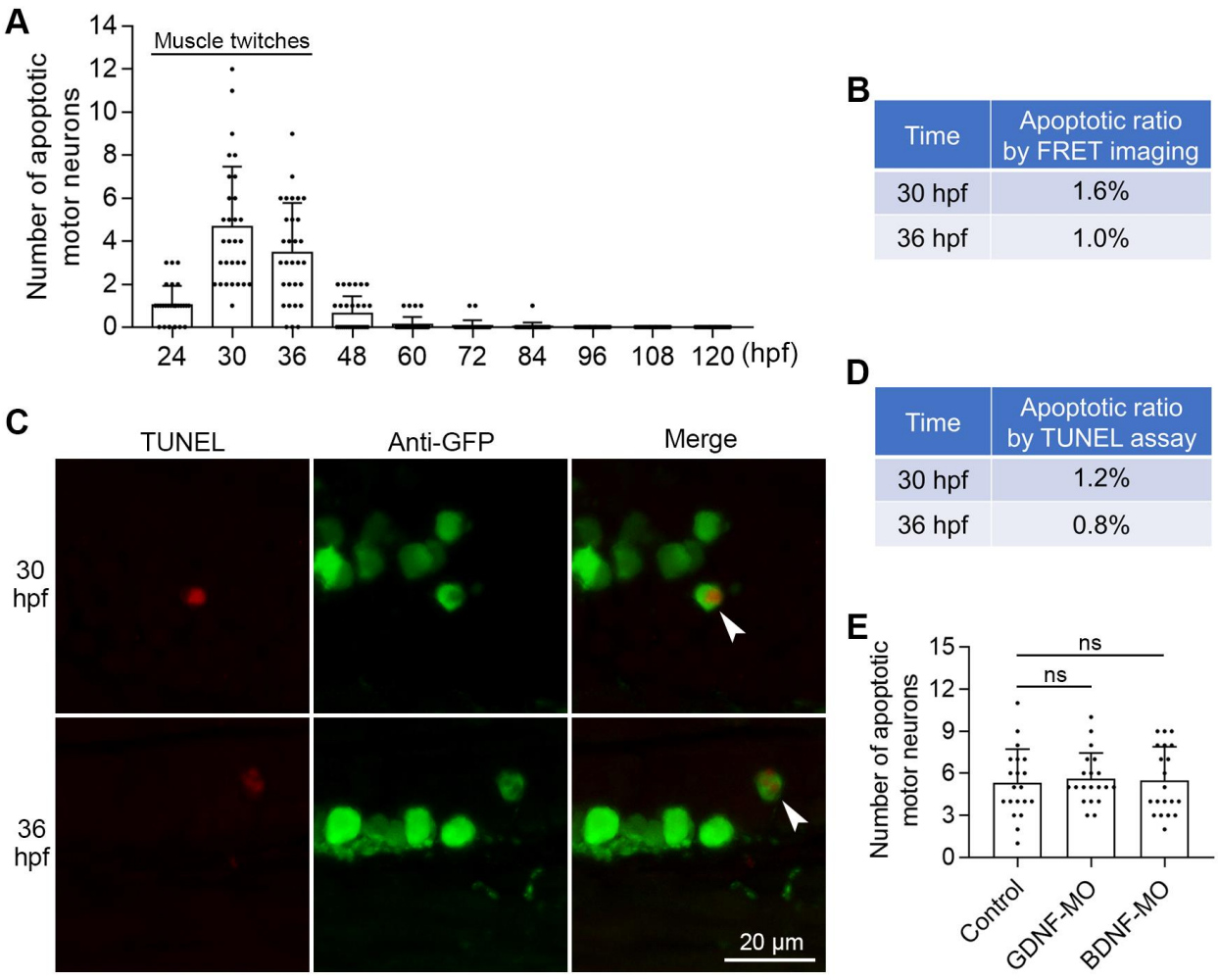

Figure 4. Only around 2% of motor neurons died during zebrafish early development. (**A**) The quantified results show the number of apoptotic motor neurons at each time point during zebrafish early development (n = 30 zebrafish for each time point). (**B**) The percentages of apoptotic motor neurons among total motor neurons at 30 hpf and 36 hpf. (**C**) TUNEL assays showing apoptotic motor neurons at 30 hpf and 36 hpf. Immunofluorescence staining with an anti-GFP antibody was used to indicate motor neurons expressing sensor C3 proteins. White arrowheads indicate TUNEL-positive motor neurons. (**D**) The percentages of apoptotic motor neurons detected by TUNEL assays. (**E**) The quantified results showing the number of apoptotic

motor neurons at 30 hpf after the knockdown of GDNF or BDNF gene using morpholinos (n = 20 zebrafish for each time point). ns, no significant difference.

Most dead motor neurons could not be engulfed by macrophages

Thus far, we have shown that sensor zebrafish can be used to detect motor neuron apoptosis. The subsequent question is how the apoptotic bodies of these dead motor neurons are removed. Macrophages are the major phagocytes to engulf apoptotic bodies in animals (Nagata & Segawa, 2021); therefore, we focused on macrophages. We fully utilized the advantages of sensor zebrafish, which label motor neurons with green fluorescence, and another transgenic zebrafish line, Tg(*mpeg1*:mCherry), which labels macrophages with a red fluorescent protein (Ellett, Pase, Hayman, Andrianopoulos, & Lieschke, 2011). Live imaging showed that red macrophages distributed everywhere in the zebrafish body at 36 hpf (Figure 5A). Interestingly, after examining 164 apoptotic motor neurons from Tg(*mnx1*:sensor C3) zebrafish, we only found one case of macrophage engulfment, in which the macrophage indicated with a yellow arrowhead was engulfing the apoptotic bodies of the axon part in the somite, which were indicated with a white arrowhead (Figure 5B). The engulfment percentage was only 0.6% (Figure 5C). These results indicated that the apoptotic bodies of dead motor neurons in the spinal cord were not cleared by macrophages.

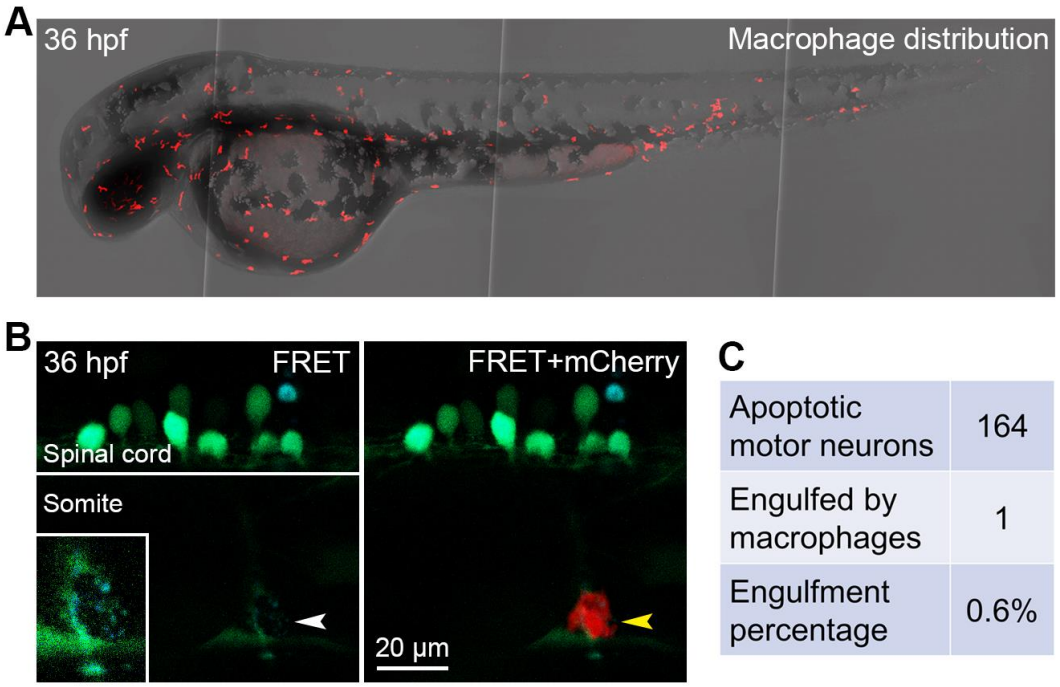

Apoptotic motor neurons	164
Engulfed by macrophages	1
Engulfment percentage	0.6%

Figure 5. Most dead motor neurons could not be engulfed by macrophages. (**A**) Live imaging showing the distribution of macrophages in zebrafish body at 36 hpf. (**B**) An example showing the engulfment of apoptotic bodies derived from the axon of a motor neuron by a macrophage in a somite at 36 hpf. The apoptotic bodies are indicated with a white arrowhead and enlarged in the box in the left image. The engulfment by the macrophage is indicated with a yellow arrowhead in the right image. The anatomical structures are indicated. (**C**) The percentage of apoptotic motor neurons engulfed by macrophages. The total number of apoptotic motor neurons observed, and the number of engulfed apoptotic motor neurons are listed.

Discussion

By expressing FRET-based sensor C3 in zebrafish, for the first time, we were able to monitor the whole process of caspase-3 activation in single motor neurons and the subsequent breakdown of these dead neurons into apoptotic bodies during development. We found that caspase-3 was

activated within 5-6 min in an individual apoptotic motor neuron, while the caspase-3 in the rest of the neurons in the same bundle was not activated. More importantly, within the same motor neuron, although the cell body is located in the spinal cord and the axon is extended into the muscle tissue, the caspase-3 activation occurred almost at the same time of observation. These data indicate a synchronized activation pattern of caspase-3 in apoptotic motor neurons.

It is generally accepted that during the development of vertebrates, approximately half of the motor neurons are removed by apoptosis. However, our results showed that motor neurons were not prone to death during early zebrafish development: only around 2% of motor neurons died of apoptosis during the early development of zebrafish. This large discrepancy may be the unique properties of zebrafish compared with chicks and rats, which could be further investigated. Another possibility is that the limitations of conventional apoptosis detection methods such as the terminal deoxynucleotidyl transferase dUTP nick end labeling (TUNEL) assay (Loo, 2011), nuclear morphology staining (H. Li et al., 2000) and caspase-3 staining (Wang et al., 2010) may potentially exaggerate the number of apoptotic cells in tissue sections. For example, the specificity of antibodies for apoptotic markers or the quality of other reagents in experiments may not be good enough, which can result in false positive apoptotic signals. Besides, these staining methods have difficulties in distinguishing neuronal cells and nearby glial cells; thus, dead glial cells may also be counted as dead neuronal cells. GDNF and BDNF are well-known neurotrophic factors for motor neurons. However, our results showed that inhibition of these two genes could not increase the death rates, which also indicated that zebrafish motor neurons were not prone to cell death during early development.

The removal of dead cells by phagocytes can effectively reduce the occurrence of inflammation, which is very important for animals (Arandjelovic & Ravichandran, 2015). Our

study showed that macrophages, although serving as professional phagocytes, could not enter the spinal cord to engulf the apoptotic motor neurons. Thus, some other cells in the spinal cord may help to engulf the dead cells. For example, a recent zebrafish study reported that neural crest cells can help to remove apoptotic cells in the nervous system during development (Zhu et al., 2019). In the future, we will investigate whether red fluorescent protein-labeled neural crest cells could engulf dead motor neurons in our sensor zebrafish.

During the past several decades, the real-time tracking of neuronal cell apoptosis under physiological conditions in live animals remains challenging. Since the development of fluorescent proteins, several FRET-based protein biosensors have been designed for the detection of apoptosis in live cells cultured in petri dishes (Ai, Hazelwood, Davidson, & Campbell, 2008; Albeck et al., 2008; Karasawa, Araki, Nagai, Mizuno, & Miyawaki, 2004; Mahajan, Harrison-Shostak, Michaux, & Herman, 1999; Rehm et al., 2002; Tyas, Brophy, Pope, Rivett, & Tavaré, 2000; Xu et al., 1998). However, unlike the good performances of these biosensors *in vitro*, the *in vivo* applications of these biosensors have been unsatisfactory because of their small dynamic ranges and the complex optical environments in live animals (Andrews et al., 2016; Takemoto et al., 2007; Takemoto, Nagai, Miyawaki, & Miura, 2003; Yamaguchi et al., 2011). We compared sensor C3 with other FRET-based apoptotic biosensors and found that sensor C3 can achieve a FRET effect of 4- to 5-fold, while other biosensors usually had FRET effects of less than or near 2-fold. This high FRET effect makes sensor C3 the ideal biosensor for visualizing neuronal cell apoptosis in live animals where other biosensors encounter difficulties.

In summary, our results showed that sensor zebrafish can serve as valuable tools for studying motor neuron apoptosis in live zebrafish, which could improve our understanding of neuronal cell apoptosis during normal development and in neurodegenerative diseases.

Materials and methods

Zebrafish maintenance

Zebrafish (AB strain) were raised at 28 °C in a ZebTEC system. The photoperiod was 14 h of light and 10 h of darkness. Zebrafish were fed with artemia twice a day. The experiments in this study were approved by the Animal Research Ethics Committee of the University of Macau (Protocol ID: UMARE-032-2016).

Generation of sensor zebrafish

The zebrafish genome was extracted using the DNeasy Blood & Tissue Kit (Qiagen, 69504). A zebrafish motor neuron-specific promoter *mnx1* was amplified by polymerase chain reaction (forward primer, ACGCGTCGACGAATTCATTTAAATTAGCCTGGCATC, reverse primer, CCCACCGGTCTGGCCCACCTCACAAACAGATTA). The promoter sequence and sensor C3 gene were cloned into the same plasmid backbone to generate the transgenic vector, named pSK-*mnx1*-C3. *Tol2* mRNA was obtained by *in vitro* transcription using the mMESSAGE mMACHINE SP6 transcription kit (Ambion, AM1340). The transgenic vector containing the sensor C3 gene (final concentration, 50 ng/μL) and *Tol2* mRNA (final concentration, 100 ng/μL) were mixed and injected (2-4 nL) into newly fertilized zebrafish eggs using an MPPI-3 pressure injector. The zebrafish embryos with green fluorescence indicating sensor C3 expression were selected under a stereomicroscope with a GFP filter. These positive zebrafish were cultured to sexual maturity and crossed with wild-type zebrafish to obtain transgenic sensor zebrafish.

In vivo FRET imaging of neuronal cell apoptosis

Sensor zebrafish embryos or larvae were anesthetized with 0.016% tricaine (Sigma-Aldrich, E10521) solution. Anesthetized zebrafish were embedded in low melting point agarose gel (Promega, V2111) in a confocal dish. The zebrafish were then imaged using a Carl Zeiss LSM 710 or LSM880 confocal laser scanning microscope. For FRET imaging, a 458 nm laser was used to excite sensor C3 proteins, and the emissions were collected simultaneously in two channels: 460-500 nm was collected as the CFP channel, designated as blue, and 520-550 nm was collected as the YFP channel, designated as green. Then, the CFP and YFP images were merged to generate the FRET images. In live neuronal cells, sensor C3 emitted green fluorescence when CFP was excited because of the energy transfer from CFP to YFP, while in apoptotic neuronal cells, activated caspase-3 proteins cleaved sensor C3 at the DEVD site, and the FRET effect was abolished. Thus, sensor C3 emitted blue fluorescence when CFP was excited under the same condition.

Immunofluorescence and TUNEL assay

Tg(*mnx1*:sensor C3) zebrafish were fixed in 4% paraformaldehyde at 4 °C for 12 h. The fixed zebrafish were dehydrated in 30% sucrose at 4 °C for 48 h. The zebrafish were then embedded in Shandon Cryomatrix embedding resin (Thermo Scientific, 6769006), and frozen sections were cut at 25 μm using a Leica CM3050S cryostat. The sections were washed with phosphate-buffered saline (PBS) three times to remove the embedding resin and then were blocked with 1% bovine serum albumin with 0.1% Triton X-100 in PBS for 1 h at room temperature (RT). Then, the sections were coated with anti-GFP primary antibody (Cell Signaling, 2956, 1:400) for 2 h at

RT. After that, the sections were washed with PBS three times and then coated with Alexa Fluor 488-conjugated goat anti-rabbit secondary antibody (Thermo Scientific, A-11034, 1:200) for 1 h at RT. The sections were washed with PBS three times. The terminal deoxynucleotidyl transferase and Cy3-dUTP labeling solution in the TUNEL kit (Beyotime, C1089) were mixed. The sections were then incubated with this reaction mixture for 1 h at 37 °C. After the incubation, the sections were washed with PBS three times and then mounted with Mowiol mounting medium (Millipore, 475904). The sections were imaged with a Carl Zeiss LSM880 confocal laser scanning microscope with 488 nm and 561 nm lasers.

Microinjection of morpholinos

Zebrafish eggs were collected after fertilization and were placed on an agarose plate. Approximately 5 nL morpholino (0.5 mM) specific to the GDNF gene (sequence, TGGCTAGAATGTCCCATAACTTCAT) or BDNF gene (sequence, TGGTCATCACTCTTCTAACCTGTTG) of zebrafish was injected into one-cell stage embryos using the MPPI-3 pressure injector. After injection, the zebrafish were quickly transferred into fresh fish water.

***In vivo* imaging of macrophage engulfment**

Tg(*mnx1*:sensor C3) zebrafish were crossed with Tg(*mpeg1*:mCherry) zebrafish to get offspring that neuronal cells and macrophages were labeled with green and red, respectively. The zebrafish were then imaged using a Carl Zeiss LSM880 confocal laser scanning microscope. FRET

imaging was applied to detect apoptotic neuronal cells. At the same time, a 561 nm laser was used to excite the mCherry proteins for the visualization of macrophages.

Statistical analysis

All of the data are expressed as the means ± SD. Statistical significance was judged by one- or two-way ANOVA using GraphPad Prism 7 software.

Supplementary materials

Supplementary materials can be found online.

Acknowledgments

The authors acknowledge the great support of the Animal Research Core and Biological Imaging and Stem Cell Core of the Faculty of Health Sciences at the University of Macau. The transgenic zebrafish line Tg(*mpeg1*:mCherry) was a gift from Dr. Kun Wu. This work was financially supported by the Multi-Year Research Grant of University of Macau (File no. MYRG2020-00121-FHS and MYRG2022-00025-FHS), the Science and Technology Development Fund (FDCT) of Macao (File no. 0147/2020/A3, 044/2021/APD and 0004/2021/AKP), Ministry of Education Frontiers Science Centre for Precision Oncology (File no. SP2021-00001-FSCPO and SP2023-00001-FSCPO) and an FHS Internal Project Grant of the University of Macau.

Author contributions

H.J. and K.Q.L. designed the experiments. H.J. and H.Y. performed the experiments. H.J. and K.Q.L. analyzed the data. H.J. prepared the manuscript. K.Q.L. revised the manuscript. K.Q.L. supervised the study.

Competing interests

The authors declare no competing interests.

Data and materials availability

All data needed to evaluate the conclusions in the paper are present in the paper and/or the Supplementary materials.

References

Ai, H.-w., Hazelwood, K. L., Davidson, M. W., & Campbell, R. E. (2008). Fluorescent protein FRET pairs for ratiometric imaging of dual biosensors. *Nat. Methods, 5*(5), 401-403.

Albeck, J. G., Burke, J. M., Aldridge, B. B., Zhang, M., Lauffenburger, D. A., & Sorger, P. K. (2008). Quantitative analysis of pathways controlling extrinsic apoptosis in single cells. *Mol. Cell, 30*(1), 11-25.

Anand, P., Fu, A., Teoh, S. H., & Luo, K. Q. (2015). Application of a fluorescence resonance energy transfer (FRET)-based biosensor for detection of drug-induced apoptosis in a 3D breast tumor model. *Biotechnol. Bioeng., 112*(8), 1673-1682.

Andrews, N., Ramel, M. C., Kumar, S., Alexandrov, Y., Kelly, D. J., Warren, S. C., . . . Frankel, P. (2016). Visualising apoptosis in live zebrafish using fluorescence lifetime imaging with optical projection tomography to map FRET biosensor activity in space and time. *J. Biophotonics, 9*(4), 414-424.

Arandjelovic, S., & Ravichandran, K. S. (2015). Phagocytosis of apoptotic cells in homeostasis. *Nat. Immunol., 16*(9), 907-917.

Arkhipova, V., Wendik, B., Devos, N., Ek, O., Peers, B., & Meyer, D. (2012). Characterization and regulation of the hb9/mnx1 beta-cell progenitor specific enhancer in zebrafish. *Dev. Biol., 365*(1), 290-302.

Blanquie, O., Yang, J.-W., Kilb, W., Sharopov, S., Sinning, A., & Luhmann, H. J. (2017). Electrical activity controls area-specific expression of neuronal apoptosis in the mouse developing cerebral cortex. *Elife, 6*, e27696.

Butterfield, D. A., & Halliwell, B. (2019). Oxidative stress, dysfunctional glucose metabolism and Alzheimer disease. *Nat. Rev. Neurosci., 20*(3), 148-160.

Castillo-Ruiz, A., Hite, T. A., Yakout, D. W., Rosen, T. J., & Forger, N. G. (2020). Does birth trigger cell death in the developing brain? *eNeuro, 7*(1), 1-11.

Cintrón-Colón, A. F., Almeida-Alves, G., Boynton, A. M., & Spitsbergen, J. M. (2020). GDNF synthesis, signaling, and retrograde transport in motor neurons. *Cell and Tissue Research, 382*, 47-56.

Dekkers, M. P., Nikoletopoulou, V., & Barde, Y.-A. (2013). Death of developing neurons: New insights and implications for connectivity. *J. Cell Biol., 203*(3), 385-393.

Ellett, F., Pase, L., Hayman, J. W., Andrianopoulos, A., & Lieschke, G. J. (2011). mpeg1 promoter transgenes direct macrophage-lineage expression in zebrafish. *Blood, 117*(4), e49-e56.

Fu, A., Peh, Y. M., Ngan, W., Wei, N., & Luo, K. Q. (2018). Rapid identification of antimicrometastases drugs using integrated model systems with two dimensional monolayer, three dimensional spheroids, and zebrafish xenotransplantation tumors. *Biotechnol. Bioeng., 115*(11), 2828-2843.

Fuchs, Y., & Steller, H. (2011). Programmed cell death in animal development and disease. *Cell, 147*(4), 742-758.

Hamburger, V. (1975). Cell death in the development of the lateral motor column of the chick embryo. *Journal of Comparative Neurology, 160*(4), 535-546.

Hao, M., Huang, B., Wu, R., Peng, Z., & Luo, K. Q. (2023). The Interaction between Macrophages and Triple-negative Breast Cancer Cells Induces ROS-Mediated Interleukin 1α Expression to Enhance Tumorigenesis and Metastasis. *Advanced Science*, 2302857.

Harris, A., & McCaig, C. (1984). Motoneuron death and motor unit size during embryonic development of the rat. *Journal of Neuroscience, 4*(1), 13-24.

He, Y.-Y., Zhang, X.-Y., Yung, W.-H., Zhu, J.-N., & Wang, J.-J. (2013). Role of BDNF in central motor structures and motor diseases. *Molecular Neurobiology, 48*, 783-793.

Heck, N., Golbs, A., Riedemann, T., Sun, J.-J., Lessmann, V., & Luhmann, H. J. (2008). Activity-dependent regulation of neuronal apoptosis in neonatal mouse cerebral cortex. *Cereb. Cortex, 18*(6), 1335-1349.

Hernandez-Baltazar, D., Mendoza-Garrido, M. E., & Martinez-Fong, D. (2013). Activation of GSK-3β and caspase-3 occurs in Nigral dopamine neurons during the development of apoptosis activated by a striatal injection of 6-hydroxydopamine. *PloS One, 8*(8), e70951.

Hollville, E., Romero, S. E., & Deshmukh, M. (2019). Apoptotic cell death regulation in neurons. *FEBS J., 286*(17), 3276-3298.

Jia, H., Song, Y., Huang, B., Ge, W., & Luo, K. Q. (2020). Engineered sensor zebrafish for fast detection and real-time tracking of apoptosis at single-cell resolution in live animals. *ACS Sens., 5*(3), 823-830.

Kandel, E. R., Schwartz, J. H., Jessell, T. M., Siegelbaum, S. A., & Hudspeth, A. J. (2012). *Principles of Neural Science, Fifth Edition*: McGraw-Hill New York.

Karasawa, S., Araki, T., Nagai, T., Mizuno, H., & Miyawaki, A. (2004). Cyan-emitting and orange-emitting fluorescent proteins as a donor/acceptor pair for fluorescence resonance energy transfer. *Biochem. J., 381*(1), 307-312.

Kaslin, J., & Ganz, J. (2020). Zebrafish nervous systems. In *The zebrafish in biomedical research* (pp. 181-189): Elsevier.

Kishino, A., Ishige, Y., Tatsuno, T., Nakayama, C., & Noguchi, H. (1997). BDNF prevents and reverses adult rat motor neuron degeneration and induces axonal outgrowth. *Experimental Neurology, 144*(2), 273-286.

Li, H., Kolluri, S. K., Gu, J., Dawson, M. I., Cao, X., Hobbs, P. D., . . . Lin, F. (2000). Cytochrome c release and apoptosis induced by mitochondrial targeting of nuclear orphan receptor TR3. *Science, 289*(5482), 1159-1164.

Li, K., Wu, R., Zhou, M., Tong, H., & Luo, K. Q. (2021). Desmosomal proteins of DSC2 and PKP1 promote cancer cells survival and metastasis by increasing cluster formation in circulatory system. *Sci. Adv., 7*(40), eabg7265.

Loo, D. T. (2011). In situ detection of apoptosis by the TUNEL assay: an overview of techniques. In *DNA damage detection in situ, ex vivo, in vivo* (Vol. 682, pp. 3-13): Humana Press.

Lossi, L., & Merighi, A. (2003). In vivo cellular and molecular mechanisms of neuronal apoptosis in the mammalian CNS. *Prog. Neurobiol., 69*(5), 287-312.

Luo, K. Q., Vivian, C. Y., Pu, Y., & Chang, D. C. (2001). Application of the fluorescence resonance energy transfer method for studying the dynamics of caspase-3 activation during UV-induced apoptosis in living HeLa cells. *Biochem. Biophys. Res. Commun., 283*(5), 1054-1060.

Mahajan, N. P., Harrison-Shostak, D. C., Michaux, J., & Herman, B. (1999). Novel mutant green fluorescent protein protease substrates reveal the activation of specific caspases during apoptosis. *Chem. Biol., 6*(6), 401-409.

Menelaou, E., Husbands, E. E., Pollet, R. G., Coutts, C. A., Ali, D. W., & Svoboda, K. R. (2008). Embryonic motor activity and implications for regulating motoneuron axonal pathfinding in zebrafish. *Eur. J. Neurosci, 28*(6), 1080-1096.

Michel, P. P., Hirsch, E. C., & Hunot, S. (2016). Understanding dopaminergic cell death pathways in Parkinson disease. *Neuron, 90*(4), 675-691.

Moujalled, D., Strasser, A., & Liddell, J. R. (2021). Molecular mechanisms of cell death in neurological diseases. *Cell Death Differ.*, *28*(7), 2029-2044.

Naganawa, Y., & Hirata, H. (2011). Developmental transition of touch response from slow muscle-mediated coilings to fast muscle-mediated burst swimming in zebrafish. *Dev. Biol.*, *355*(2), 194-204.

Nagata, S., & Segawa, K. (2021). Sensing and clearance of apoptotic cells. *Curr. Opin. Immunol.*, *68*, 1-8.

Oppenheim, R. W. (1981). Cell death of motoneurons in the chick embryo spinal cord. V. Evidence on the role of cell death and neuromuscular function in the formation of specific peripheral connections. *Journal of Neuroscience*, *1*(2), 141-151.

Raoul, C., Henderson, C. E., & Pettmann, B. (1999). Programmed cell death of embryonic motoneurons triggered through the Fas death receptor. *J. Cell Biol.*, *147*(5), 1049-1062.

Rehm, M., Dussmann, H., Janicke, R. U., Tavare, J. M., Kogel, D., & Prehn, J. H. (2002). Single-cell fluorescence resonance energy transfer analysis demonstrates that caspase activation during apoptosis is a rapid process: role of caspase-3. *J. Biol. Chem.*, *277*(27), 24506-24514.

Rubin, L. L. (1997). Neuronal cell death: when, why and how. *Br. Med. Bull.*, *53*(3), 617-631.

Schmidt, R., Strähle, U., & Scholpp, S. (2013). Neurogenesis in zebrafish–from embryo to adult. *J Neural development*, *8*(1), 1-13.

Takemoto, K., Kuranaga, E., Tonoki, A., Nagai, T., Miyawaki, A., & Miura, M. (2007). Local initiation of caspase activation in Drosophila salivary gland programmed cell death in vivo. *Proc. Natl. Acad. Sci. U. S. A.*, *104*(33), 13367-13372.

Takemoto, K., Nagai, T., Miyawaki, A., & Miura, M. (2003). Spatio-temporal activation of caspase revealed by indicator that is insensitive to environmental effects. *J. Cell Biol., 160*(2), 235-243.

Tian, H., Ip, L., Luo, H., Chang, D. C., & Luo, K. Q. (2007). A high throughput drug screen based on fluorescence resonance energy transfer (FRET) for anticancer activity of compounds from herbal medicine. *Br. J. Pharmacol., 150*(3), 321-334.

Tyas, L., Brophy, V. A., Pope, A., Rivett, A. J., & Tavaré, J. M. (2000). Rapid caspase-3 activation during apoptosis revealed using fluorescence-resonance energy transfer. *EMBO Rep., 1*(3), 266-270.

Wang, Q., Frolova, A. I., Purcell, S., Adastra, K., Schoeller, E., Chi, M. M., . . . Moley, K. H. (2010). Mitochondrial dysfunction and apoptosis in cumulus cells of type I diabetic mice. *PloS One, 5*(12), e15901.

Weill, C. (1991). Somatostatin (SRIF) prevents natural motoneuron cell death in embryonic chick spinal cord. *Dev. Neurosci., 13*(6), 377-381.

Wu, R., Li, K., Yuan, M., & Luo, K. Q. (2021). Nerve growth factor receptor increases the tumor growth and metastatic potential of triple-negative breast cancer cells. *Oncogene, 40*(12), 2165-2181.

Xu, X., Gerard, A. L., Huang, B. C., Anderson, D. C., Payan, D. G., & Luo, Y. (1998). Detection of programmed cell death using fluorescence energy transfer. *Nucleic Acids Res., 26*(8), 2034-2035.

Yamaguchi, Y., Shinotsuka, N., Nonomura, K., Takemoto, K., Kuida, K., Yosida, H., & Miura, M. (2011). Live imaging of apoptosis in a novel transgenic mouse highlights its role in neural tube closure. *J. Cell Biol., 195*(6), 1047-1060.

Yang, H., Jia, H., Zhao, Q., & Luo, K. Q. (2022). Visualization of natural killer cell-mediated killing of cancer cells at single-cell resolution in live zebrafish. *Biosens. Bioelectron.*, *216*, 114616.

Zhu, Y., Crowley, S. C., Latimer, A. J., Lewis, G. M., Nash, R., & Kucenas, S. (2019). Migratory neural crest cells phagocytose dead cells in the developing nervous system. *Cell*, *179*(1), 74-89.

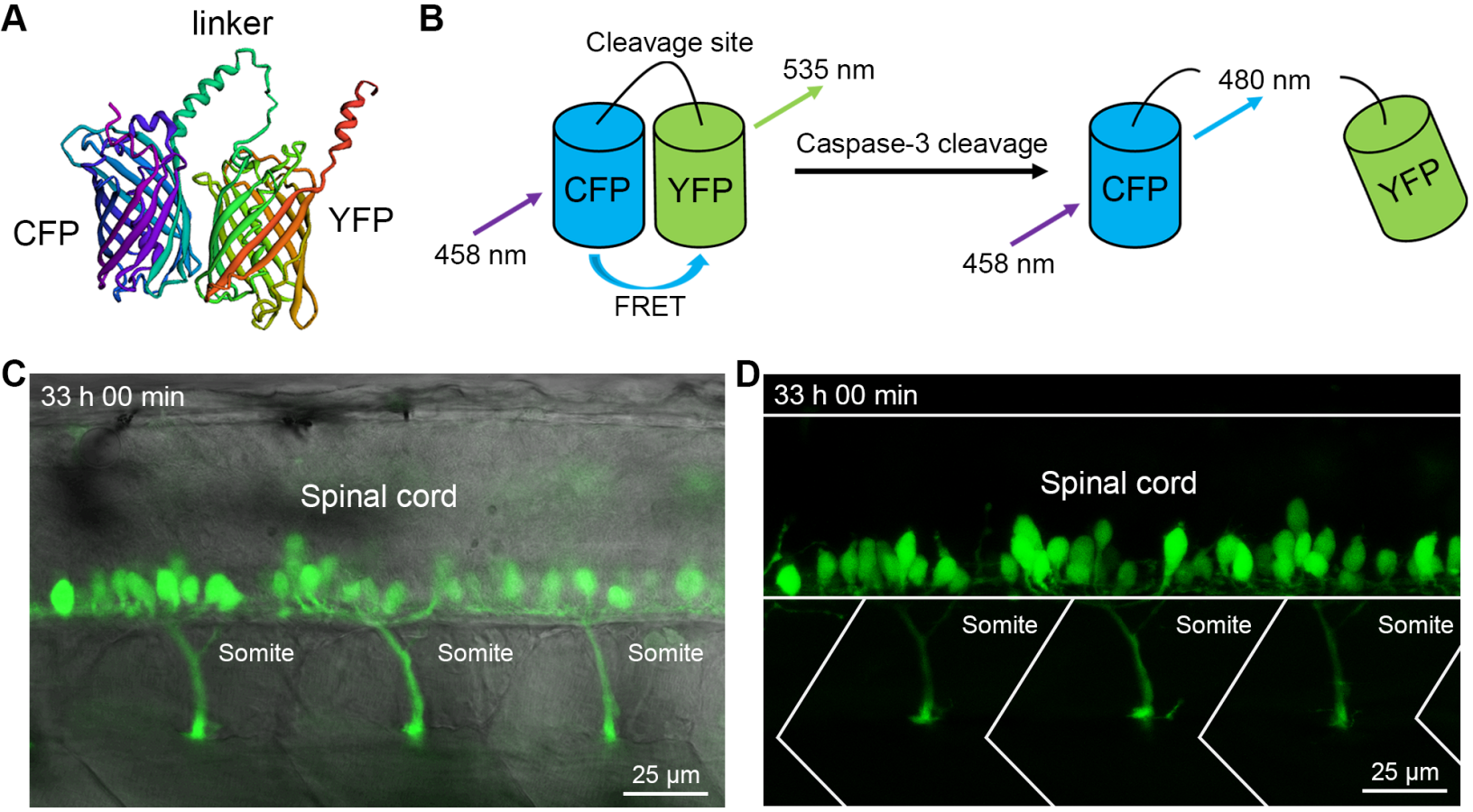
A
linker
CFP
YFP
B
Cleavage site
535 nm
CFP
YFP
458 nm
FRET
Caspase-3 cleavage
CFP
480 nm
YFP
458 nm
C
33 h 00 min
Spinal cord
Somite
Somite
Somite
25 µm
D
33 h 00 min
Spinal cord
Somite
Somite
Somite
25 µm

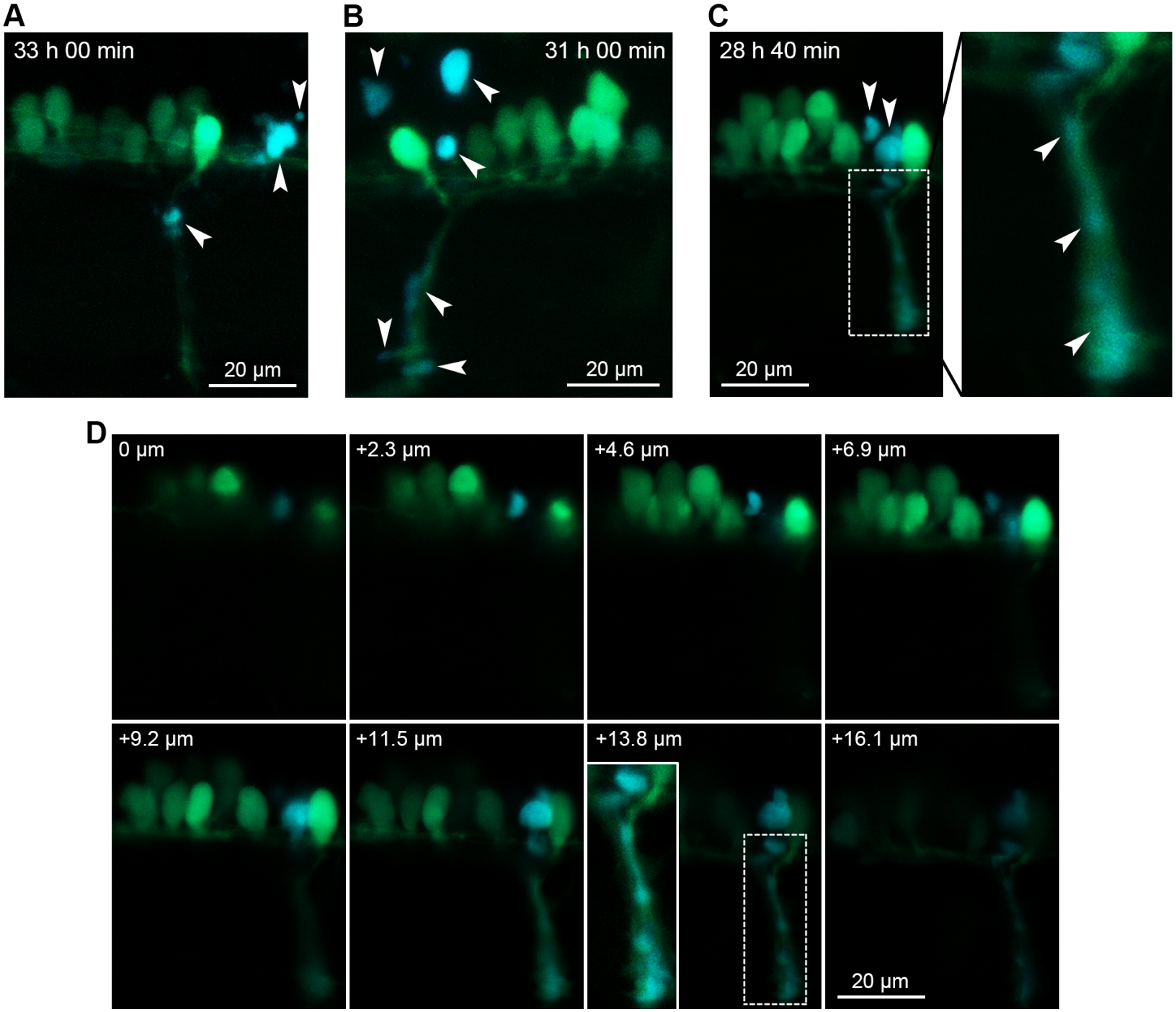
A
33 h 00 min
20 µm
B
31 h 00 min
20 µm
C
28 h 40 min
20 µm
D
0 µm
+2.3 µm
+4.6 µm
+6.9 µm
+9.2 µm
+11.5 µm
+13.8 µm
+16.1 µm
20 µm

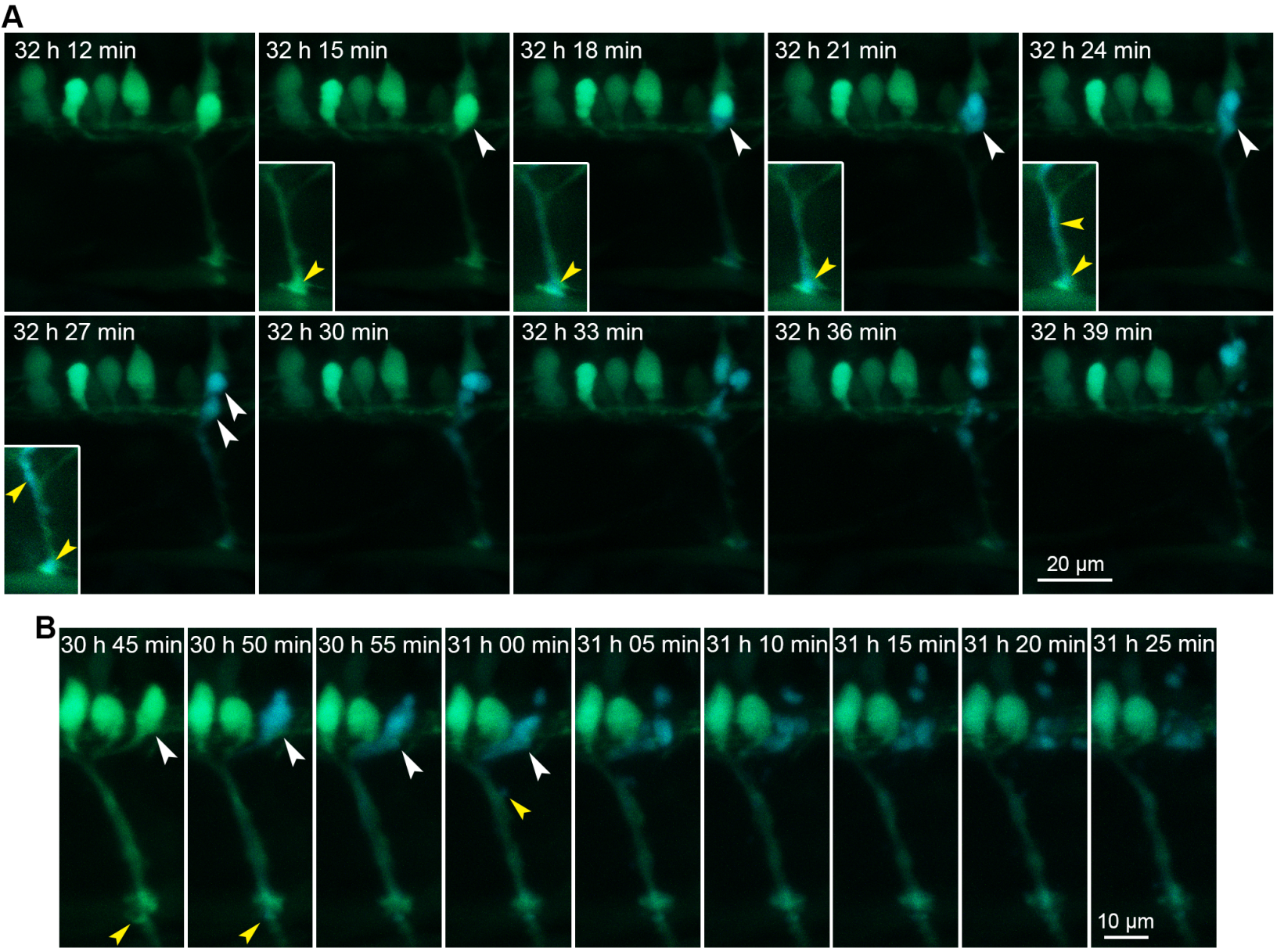
A
32 h 12 min
32 h 15 min
32 h 18 min
32 h 21 min
32 h 24 min
32 h 27 min
32 h 30 min
32 h 33 min
32 h 36 min
32 h 39 min
20 µm
B
30 h 45 min
30 h 50 min
30 h 55 min
31 h 00 min
31 h 05 min
31 h 10 min
31 h 15 min
31 h 20 min
31 h 25 min
10 µm

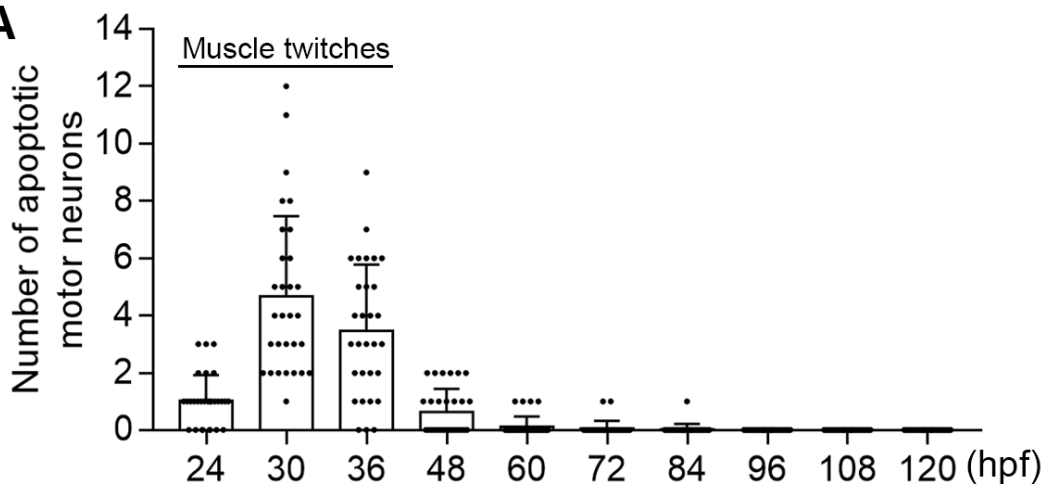

B

Time	Apoptotic ratio by FRET imaging
30 hpf	1.6%
36 hpf	1.0%

D

Time	Apoptotic ratio by TUNEL assay
30 hpf	1.2%
36 hpf	0.8%

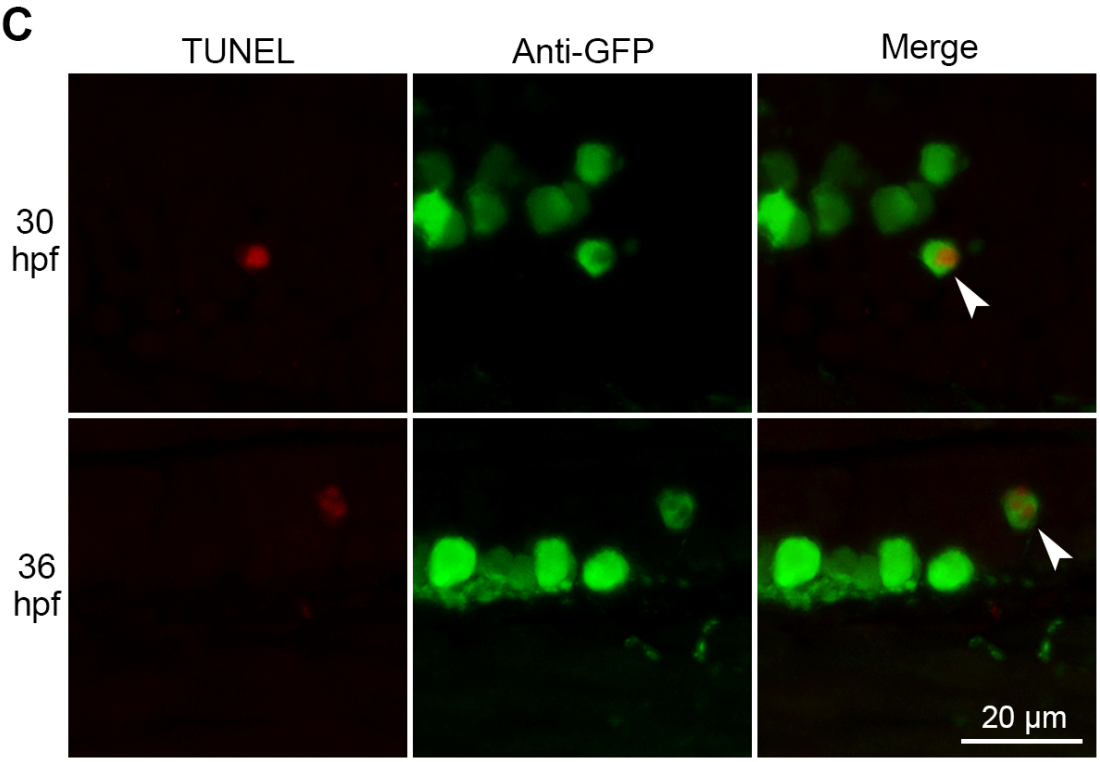

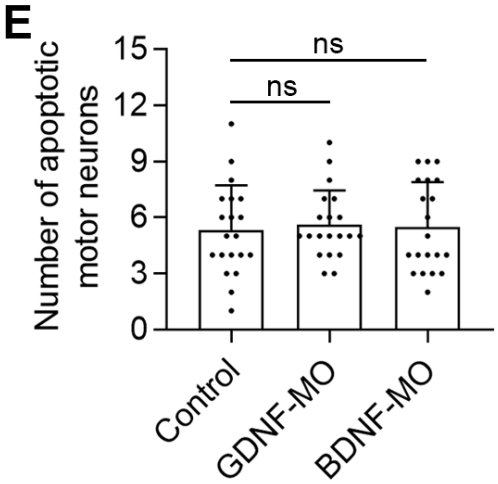

A

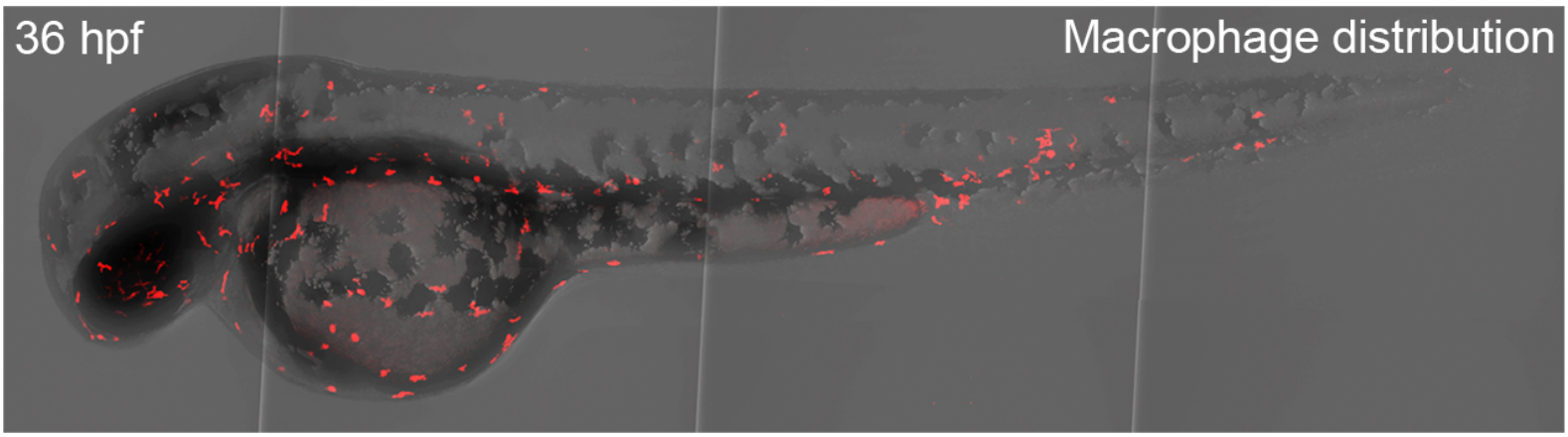

B

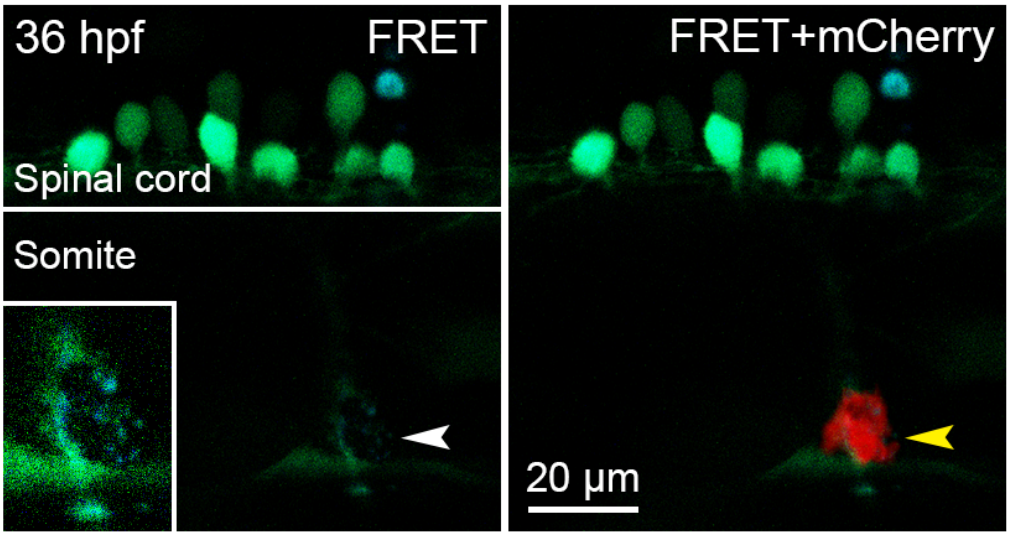

C

Apoptotic motor neurons	164
Engulfed by macrophages	1
Engulfment percentage	0.6%